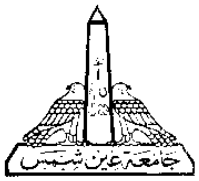

AIN SHAMS UNIVERSITY

FACULTY OF ENGINEERING

Electronics Engineering and Electrical Communications

Onboard GPS Satellite Transparent Antennas

A Thesis submitted in partial fulfilment of the requirements of the degree of

Master of Science in Electrical Engineering

(Electronics Engineering and Electrical Communications)

by

Mostafa Mahmoud Rabie Hanafy

Bachelor of Science in Electrical Engineering

(Electronics Engineering and Electrical Communications)

Faculty of Engineering, Misr International University, 2013

Supervised By

Prof. Hadia Mohamed Saeed El-Henawy

Prof. Fatma Mahmoud El-Hefnawy

Prof. Fawzy Ibrahim Abdelghany

Cairo - (2018)

AIN SHAMS UNIVERSITY

FACULTY OF ENGINEERING

Electronics and Communications

Onboard GPS Satellite Transparent Antennas

by

Mostafa Mahmoud Rabie Hanafy

Bachelor of Science in Electrical Engineering

(Electronics Engineering and Electrical Communications)

Faculty of Engineering, Misr International University, 2013

Examiners' Committee

Name and Affiliation	**Signature**
Prof. Choose an item., University	…….
Prof. Choose an item., University	…….
Dr. Choose an item., University	…….

Date: 11 July 2018

Statement

This thesis is submitted as a partial fulfilment of Master of Science in Electrical Engineering, Faculty of Engineering, Ain Shams University.

The author carried out the work included in this thesis, and no part of it has been submitted for a degree or a qualification at any other scientific entity.

Mostafa Mahmoud Rabie Hanafy

Signature

……...…….

Date: 11 July 2018

Researcher Data

Name	: Mostafa Mahmoud Rabie Hanafy
Date of birth	: 7/6/1991
Place of birth	: Cairo, Egypt
Last academic degree	: Bachelor of Science in Electrical Engineering
Field of specialization	: Electronics Engineering and Electrical Communication
University issued the degree	: Misr International University
Date of issued degree	: 9/7/2013
Current job	: Teaching Assistant at Misr International University

Abstract (Thesis Summary)

The main objective in this Thesis is to design, simulate, fabricate, lab measure and result analysis of a microstrip transparent antenna for Cubesat satellites to communicate with the MEO orbit GPS constellation and to fulfill the following specification requirements:

Frequency: GPS L1 band (1.575 GHz) and then transformed to GPS L2 band (1.227 GHz), Bandwidth (BW) > 50 MHz, Circular Polarization with Axial Ratio (AR) ≤ 3 dB, Radiation Pattern: Gain (G) > 5 dBi , 3dB beamwidth > 60°, Small reflection coefficient (Return loss) ≤ -10 dB, Power handling Capability > 2W, 1 port 50 ohm SMA female standard connector, Small size and low weight, Low profile, Percentage of Transparency (PT) > 60%.

In this thesis an introduction to the history of Cubesats and its required antennas, also the motivations, problem statement, project phases and report organization are introduced in Chapter 1. Literature survey about Cubesats, there different types of antennas, transparent antenna techniques, GPS and its antenna requirements are introduced in Chapter 2.

Three transparent GPS microstrip antenna designs are introduced in this thesis.

In Chapter 3, two antennas are designed using transparent substrates (Quartz and Pyrex Glass), to show a variety of different substrates that can be used in the transparent antenna design. The two antennas are designed to operate at the GPS L1 band (f_r = 1.575 GHz) and then frequency transformed to operate at the GPS L2 band (f_r = 1.227 GHz). These antennas are simulated using Computer Simulation Technology, CST. The L1 band Quartz MSA achieves Return Loss (S11) of -15.7 dB, bandwidth, BW of 64.7 MHz (4.12 % of f_r), gain of 6.052 dBi, efficiency, e_0 of 96.45 %, Axial Ratio of 3.5 dB and Percentage of Transparency (PT) of 61 %. The L1 band Pyrex Glass MSA achieves Return Loss (S11) of -18.3 dB, bandwidth, BW of 107 MHz (6.8 % of f_r), gain of 4.7 dBi, efficiency, e_0 of 98 %, Axial Ratio of 2.9 dB and Percentage of

Transparency (PT) of 90 %. The L2 band Quartz MSA achieves Return Loss (S11) of -15.8 dB, bandwidth, BW of 48 MHz (3.91 % of f_r), gain of 5.733 dBi, efficiency, e_0 of 96.57 %, Axial Ratio of 3.9 dB and Percentage of Transparency (PT) of 61 %. The L2 band Pyrex Glass MSA achieves Return Loss (S11) of -16.333 dB, bandwidth, BW of 73 MHz (5.94 % of f_r), gain of 4.45 dBi, efficiency, e_0 of 95.97 %, Axial Ratio of 3.3 dB and Percentage of Transparency (PT) of 90 %.

In Chapter 4, the third antenna is designed using a nontransparent substrate (Rogers RT/duroid 5880), however achieving transparency. The third design gives the flexibility of choosing any type of substrates, without losing the transparency of the antenna. In other words a transparent antenna can be designed without any material limitations. This antenna is designed to operate at the GPS L1 band (f_r = 1.575 GHz) and then frequency transformed to operate at the GPS L2 band (f_r = 1.227 GHz). The antenna is simulated using Computer Simulation Technology, CST. The L1 band Rogers RT/duroid 5880 MSA achieves Return Loss (S11) of -45.83 dB, bandwidth, BW of 60 MHz (3.82 % of f_r), gain of 6.687 dBi, efficiency, e_0 of 97.5 %, Axial Ratio of 3 dB and Percentage of Transparency (PT) of 71.5 %. The L2 band Rogers RT/duroid 5880 MSA achieves Return Loss (S11) of -25.64 dB, bandwidth, BW of 40.8 MHz (3.33 % of f_r), gain of 6.15 dBi, efficiency, e_0 of 95.04 %, Axial Ratio of 2.9 dB and Percentage of Transparency (PT) of 71.5 %. Temperature analysis is performed on the three antennas designed in this thesis at operating frequency (f_r = 1.575 GHz), to test their performance in the outer space. The parameters of the three L1 band antennas designed in this thesis as well as the parameters of their three transformed L2 band versions are analyzed and compared, using a Performance Indicator (PI) and a Performance Metric (PM). The Rogers RT/duroid 5880 L1 band antenna is then fabricated at the National Telecommunications Institute, NTI. Lab measurements of the fabricated antenna are performed using Vector Network Analyzer (VNA) and further parameter measurements are performed using the Anechoic Chamber at the

Microwave and Antenna Research Lab, Ain Shams University. The fabricated MSA achieves Return Loss (S11) of -15 dB at f_r = 1.48 GHz with percentage of error of about 6 % in resonance frequency (f_r), bandwidth, BW of 60 MHz, gain of 5.65 dBi, efficiency, e_0 of 75 % and Percentage of Transparency (PT) of 71.5 %. Antenna parameters obtained from lab measurements are compared with that obtained from simulations and the results are analyzed.

Finally the conclusions and future work are introduced in Chapter 5.

Key words: Microstrip Antenna, Circular Polarization, Global Positioning System (GPS), Transparent Antenna, Cube satellites, Cubesats.

Acknowledgements

It would not have been possible to write this thesis without the help and support of the great people around me, to only some of whom it is possible to give particular mention here.

This thesis would not have been possible without the help, support and patience of my supervisors, Prof. Hadia El-Henawy, Prof. Fatma El-Hefnawy**,** and Prof. Fawzy Ibrahim, not to mention their guidance, unsurpassed knowledge, good advice and support.

Beside my advisors, i would like to acknowledge the academic support of the rest of Electronics and Communication Engineering department in Ain Shams University (ASU) and Misr International University (MIU).

Last but not least, i would like to thank my family for their great support throughout my education.

July 2018

Table of Contents

List of Figures ii
List of Tables viii
List of Abbreviations x
List of Symbols xi
Chapter 1 Introduction. 1
1.1 Introduction to MSA for Cubesat applications 1
1.2 Motivation 2
1.3 Problem Statement 3
1.4 Thesis Phases 3
1.5 Thesis Organization 3
Chapter 2 Review on Cubesat, Transparent Antennas and GPS Antennas 5
2.1 Introduction to Cubesat 5
2.1.1 History of Cubesat antennas 6
2.2 Transparent MSA 9
2.4 Reviews on Global Positioning System (GPS) Antennas 15
2.4.1 History of GPS 15
2.4.2 Global Positioning System (GPS) MSA 16
2.4.3 Polarization of GPS MSA 16
2.4.4 Review on Previously Designed Circularly Polarized GPS MSAs 18
Chapter 3 Transparent L1 band GPS MSA and Frequency Transformation to L2 band 20
3.1 Introduction 20
3.2 Transparent Meshed MSA Concept 21
3.2.1 Structure 21
3.2 Transparency Control and Measurement 22
3.3 Design of Non-transparent Rectangular MSA 23
3.3.1 Substrate selection 23
3.3.2 Initial Design of Rectangular MSA 25
3.3.3 Optimization of Rectangular MSA 27

3.3.4 Circular Polarization of the Non-transparent Designed Antenna 32
3.4 Design of Transparent MSA on Quartz Substrate 36
3.4.1 Design of Meshed MSA on Quartz Substrate. 36
3.4.2 Optimized Meshed MSA on Quartz Substrate at 1.575 GHz results 37
3.5 Design of Transparent MSA on Pyrex Glass Substrate 43
3.5.1 Design of Meshed MSA on Pyrex Glass Substrate 43
3.5.2 Optimized Meshed MSA on Pyrex Glass Substrate 44
3.6 Frequency Transformation to Design L2 Band Transparent MSA 49
3.6.1 Generic Transformation for Single Band Antenna 49
3.6.2 Application of Frequency Transformation on Quartz Substrate MSA. 50
3.6.3 Application of Frequency Transformation on Pyrex Glass substrate MSA 58
3.7 Results Analysis 65
Chapter 4 Meshed Conductor and Meshed Substrate MSA 67
4.1 Introduction 67
4.2 Structure of Meshed Conductor Meshed Substrate GPS MSA 68
4.3 Design of Meshed Conductor Meshed Substrate L1 band GPS Antenna 73
4.3.1 Substrate selection 74
4.3.2 Transparency Control and Measurement 74
4.3.3 Initial Design Meshed Conductor Meshed Substrate L1 Band Antenna 76
4.3.4 Optimized Meshed Conductor Meshed Substrate L1 Band Antenna 77
4.4 Effect of Space Temperature Variation on the Designed Antennas 82
4.4.1 Temperature variation for transparent MSA with transparent Quartz substrate 85
4.4.2 Temperature variation for transparent MSA with Pyrex Glass substrate 88
4.4.3 Temperature variation for transparent meshed conductor meshed substrate MSA. 92
4.5 Result Analysis and Comparison 96

4.6 Fabrication and lab Measurements of Meshed Conductor Meshed Substrate Antenna 101
4.7 Frequency Transformation of the Meshed Conductor Meshed Substrate MSA. 108
4.7.1 Generic Transformation for the Meshed Conductor Meshed Substrate MSA..... 108
4.7.2 Simulation of Transformed Meshed Conductor Meshed Substrate GPS L2 Band MSA 108
4.4.3 Transformed MSAs Comparison..... 113
4.8 Result Analysis..... 115
Chapter 5 Conclusions and Future Work..... 118
5.1 Thesis Conclusions..... 118
5.2 Future Work 121
References..... 122
Publications..... 129

List of Figures

Fig. 1.1 One Unit Cubesat 2
Fig. 1.2 Three Units MBD Cubesat 2

Fig. 2.1 Cubesat's architecture and subsystem labels [4] 8
Fig. 2.2 ISARA Cubesat [10] 8
Fig. 2.3 MarCO Cubesat [10] 9
Fig. 2.4 The Bull's Eye antenna [10] 9
Fig. 2.5 The slatted ring resonator antenna on a Cubesat chassis 10
Fig. 2.6 Meshed patch antenna: (a) Rectangular (b) Circular 11
Fig. 2.7 MEO GPS constellation of satellites 16
Fig. 2.8 Circularly Polarized (CP) GPS signal 18
Fig. 2.9 GPS MSA communicating with four MEO GPS satellites 19

Fig. 3.1 Patch material gridding with N = M = 4 21
Fig. 3.2 Non-transparent rectangular MSA 25
Fig. 3.4 Optimized non-transparent rectangular MSA 28
Fig. 3.5 S11parameter (Return Loss) for the optimized feed location and dimensions non-transparent MSA 29
Fig. 3.6 VSWR for the optimized feed location and dimensions non-transparent MSA 29
Fig. 3.7 Axial Ratio for the optimized feed location and dimensions non-transparent MSA 30
Fig. 3.8 Non-transparent microstrip GPS antenna radiation pattern 3D plot 30
Fig. 3.9 Non-transparent microstrip GPS antenna radiation pattern polar plot 31
Fig. 3.10 Antenna gain for the optimized feed location and dimensions non-transparent MSA 31

Fig. 3.11 Surface current distribution for the optimized feed location and dimensions non-transparent MSA 32
Fig. 3.12 Dually-fed circular polarization antennas (a) Branch-line hybrid fed patch (b) cross-fed patch 33
Fig. 3.13 Types of perturbed patches to achieve CP using single probe feeding [42] 34
Fig. 3.14 Truncated edges non-transparent MSA 35
Fig. 3.15 Axial Ratio for Truncated edges non-transparent MSA 35
Fig. 3.16 S11 (Return Loss) for the meshed MSA 37
Fig. 3.17 Transparent Quartz MSA, (a) front view, and (b) back view 38
Fig. 3.18 S11 for the optimized Quartz transparent MSA 39
Fig. 3.19 VSWR for the optimized Quartz transparent MSA 39
Fig. 3.20 Transparent Quartz MSA radiation pattern 3D plot 40
Fig. 3.21 Transparent Quartz MSA radiation pattern polar plot 40
Fig. 3.22 Gain for the optimized transparent Quartz MSA 41
Fig. 3.23 Axial Ratio for the optimized Quartz transparent MSA 41
Fig. 3.24 Surface current for the optimized Quartz transparent MSA 42
Fig. 3.25 Transparent meshed GPS MSA on Pyrex Glass at 1.575 GHz, (a) front view, and (b) back view 44
Fig. 3.26 S11 (Return Loss) for the optimized transparent Pyrex Glass MSA .. 45
Fig. 3.27 Transparent Pyrex Glass MSA 3D radiation pattern 45
Fig. 3.28 Transparent Pyrex Glass MSA radiation pattern polar plot 46
Fig. 3.29 Antenna gain for the optimized transparent Pyrex Glass MSA 46
Fig. 3.30 Axial Ratio for the optimized transparent Pyrex Glass MSA 47
Fig. 3.31 Surface current for the optimized transparent Pyrex Glass MSA 47
Fig. 3.32 S11 parameter of the designed transparent Quartz MSA at operating frequency 1.213 GHz 52
Fig. 3.33 S11 parameter of the optimized transparent Quartz MSA at operating frequency 1.227 GHz 52

Fig. 3.34 VSWR for the transparent Quartz MSA at operating frequency 1.227 GHz 53
Fig. 3.35 Transparent Quartz MSA at operating frequency 1.227 GHz radiation pattern 3D plot 54
Fig. 3.36 Transparent Quartz MSA at operating frequency 1.227 GHz radiation pattern polar plot 54
Fig. 3.37 Gain of the transparent Quartz MSA at operating frequency 1.227 GHz 55
Fig. 3.38 Axial Ratio of the transparent Quartz MSA at operating frequency 1.227 GHz 55
Fig. 3.39 Meshed transparent MSA with two opened slots antenna 56
Fig. 3.40 Axial Ratio of transparent Quartz MSA with two opened slots 56
Fig. 3.41 Surface current of the L2 band optimized antenna on Quartz substrate 57
Fig. 3.42 S11 parameter of the transparent Pyrex Glass MSA at operating frequency 1.227 GHz 60
Fig. 3.43 VSWR of the transparent Pyrex Glass MSA at operating frequency 1.227 GHz 60
Fig. 3.44 Transparent Pyrex Glass MSA at operating frequency 1.227 GHz radiation pattern 3D plot 61
Fig. 3.45 Transparent Pyrex Glass MSA at operating frequency 1.227 GHz radiation pattern polar plot 61
Fig. 3.46 Gain of the transparent Pyrex Glass MSA at operating frequency 1.227 GHz 62
Fig. 3.47 Axial Ratio of the of the transparent Pyrex Glass MSA at operating frequency 1.227 GHz 62
Fig. 3.48 Surface current of the optimized meshed antenna on Pyrex Glass substrate at operating frequency 1.227 GHz 63

Fig. 4.1 Meshed conductor meshed substrate transparent MSA. (a) Front view, (b) back view..... 70
Fig. 4.2 Meshed conductor meshed substrate transparent MSA side view 71
Fig. 4.3 Substrate divided into two parts each of thickness h/2..... 71
Fig. 4.4 Meshed conductor meshed substrate transparent MSA patch with dimensions L_p x W_p, (N = M = 12)..... 72
Fig. 4.5 Meshed conductor meshed substrate transparent MSA substrate with two parts identically like patch and ground 72
Fig. 4.6 Meshed conductor meshed substrate transparent MSA Ground with dimensions L_g x W_g, (N_g = M_g = 12) 73
Fig. 4.7 S11 for the initial design of meshed conductor meshed substrate transparent MSA 76
Fig. 4.8 S11 for the optimized meshed conductor meshed substrate transparent MSA..... 78
Fig. 4.9 VSWR for the optimized meshed conductor meshed substrate transparent MSA 78
Fig. 4.10 Radiation Pattern 3D plot for the optimized meshed conductor meshed substrate transparent MSA..... 79
Fig. 4.11 Radiation Pattern polar plot for the optimized meshed conductor meshed substrate transparent MSA..... 80
Fig. 4.12 Antenna gain for the optimized meshed conductor meshed substrate transparent MSA 80
Fig. 4.13 Axial Ratio for the optimized meshed conductor meshed substrate transparent MSA 81
Fig. 4.14 Surface current distribution for the optimized meshed conductor meshed substrate transparent MSA at 1.575 GHz 81
Fig. 4.15 S11 parameter of the transparent antenna with Quartz substrate at different temperatures from -60 ^{o}C to 120 ^{o}C 86
Fig. 4.16 Gain of the transparent antenna with Quartz substrate at different temperatures from -60 ^{o}C to 120 ^{o}C..... 87